

Vibration control of coupled wind tower-nacelle-blade system

Zenon J. G. Del Prado¹, Yuri L. D. Martins¹, Suzana M. Ávila², Marcus V. G. de Moraes²

¹*School of Civil and Environmental Engineering, Federal University of Goiás
Avenida Universitária, 74605-220, Goiânia/ GO, Brazil
zenon@ufg.br, yuriluzdmartins@discente.ufg.br*

²*Material Integrity Graduate program, Campus UnB Gama
12 Setor Leste, CEP 72444-240, Gama, DF, Brazil
avilas@unb.br, mvmoraes@unb.br*

Abstract. In this work, the vibration control of a coupled wind tower – nacelle – blades system subjected to external lateral loads and rotating blades is studied. To model the tower and blades, the non-linear Euler-Bernoulli beam theory and the linear Euler-Bernoulli beam, respectively, are considered. The structural control device studied is an inverted pendulum tuned mass damper (IPTMD) located at the top of the tower. The Rayleigh-Ritz method, together with Hamilton principle, is applied to obtain a set of nonlinear ordinary differential equations of motion which are, in turn, solved by the Runge-Kutta method. First, the dynamic instability is studied when rotating blades are considered, where it is possible to observe veering phenomena. In addition, the optimum parameters of the IPTMD are obtained. The results show a good performance achieved by the vibration control adopted to the dynamical behavior.

Keywords: Vibration control, tuned mass damper, inverted pendulum, dynamic instability.

1 Introduction

Slender structures such as wind towers, are very flexible and can experience large displacements when subjected to dynamical external forces considering the occurrence of coupling between tower and blades. One important way to reduce such excessive vibrations is to apply vibration control to these structures. One alternative vibration control device is the tuned mass damper (TMD), which is capable of absorbing some of the structural vibration energy, thus reducing vibration of the main structure (Song and Dargush [1]). The TMD is usually a spring-mass-damper system and its influence in wind turbines was investigated by several authors such as Murtagh *et al.* [2], Farsadi and Kayran [3], Zuo, Bi and Hao [4].

However, the TMD may have a pendular shape as studied by Orlando [5], Guimarães, Moraes and Avila [6], Sun and Jahangiri [7]. The pendulum geometry has practical advantages since its frequency can be tuned changing the cable length. In this work, an inverted pendulum geometry is considered. This geometry has already shown good results in previous studies such as in Resende, Moraes and Avila [8], where they performed an experimental-numerical study of the inverted pendulum performance in a one-degree-of-freedom structure.

The wind turbine is composed of a tower coupled to the nacelle and rotating blades at the top. The mathematical model studied both tower and blades using the non-linear Euler-Bernoulli beam theory. Then, the Rayleigh-Ritz method, together with Hamilton principle, is applied to study the structure response.

2 Mathematical formulation

The tower-nacelle-blade system model is shown in Fig. 1. The tower has height H , density ρ_T , area A_T , Young's modulus E_T , moment of inertia I_T , z is the spatial coordinate along the length and $v(z, t)$ is the tower

transverse displacement. The blade has length L , density ρ , area A , Young's modulus E , moment of inertia I and rotates with speed Ω ; x is the spatial coordinate and $u(x, t)$ the transverse displacement. At the top of the tower, there is a tip mass M_0 representing the nacelle. The system is subjected to external lateral load $F_v(t)$.

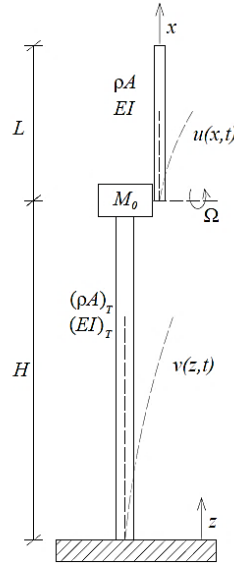


Figure 1. Wind turbine model

2.1 Energy Functional

The strain energy for the tower-blade system is given by (Orlando [5] and Kang [9]):

$$U = \int_0^H \frac{1}{2} E_T I_T \left(v_{,zz}^2 + v_{,zz}^2 v_{,z}^2 + \frac{1}{4} v_{,zz}^2 v_{,z}^4 \right) dz + \int_0^L \frac{1}{2} EI \left(u_{,xx}^2 + u_{,xx}^2 u_{,x}^2 + \frac{1}{4} u_{,xx}^2 u_{,x}^4 \right) dx \quad (1)$$

An external harmonic force is applied at the top of the tower, where F is the amplitude of the force and ω_f is the frequency of the force. Thus, the work done by this force can be expressed as.

$$W_T = -F \sin(\omega_f t) v(z, t) \Big|_{z=H} \quad (2)$$

In addition, since the blade rotates with a frequency Ω , it is necessary to consider a centrifugal force (F_c) at the blade. This force acts along the blade's length and using the dummy variable s , Meirovitch [10] proposed equation (3) to calculate it, the work done by this force is given by equation (4).

$$F_c(x) = \int_x^L \rho A s \Omega^2 ds \quad (3)$$

$$W = - \int_0^L F_c(x) \left(\frac{1}{2} \left(\frac{du}{dx} \right)^2 + \frac{1}{8} \left(\frac{du}{dx} \right)^4 \right) dx \quad (4)$$

In order to obtain the energy functional, the kinetic energy of both blade and tower has to be defined. Only the translational kinetic energy is considered, thus is given by:

$$T = \int_0^H \frac{1}{2} \rho_T A_T \left(\frac{\partial v(z, t)}{\partial t} \right)^2 dz + \frac{1}{2} M_0 \left(\frac{\partial v(z, t)}{\partial t} \right)^2 \Big|_{z=H} + \int_0^L \frac{1}{2} \rho A \left(\frac{\partial u(x, t)}{\partial t} \right)^2 dx \quad (5)$$

The boundary conditions of the tower and blade are the same of a cantilever beam, therefore displacement

and slope are zero at one end and at the other end shear force and moment are zero. Though, due to the coupling between blade and tower, a shear force appears in this region. The work W_{ac} of this force can be calculated by equation (6), furthermore, it is important to note that the blade displacement is relative to the tower displacement, since the blade is fixed to the end-tip of the tower, as shown by equation (7), which changes the expression for the kinetic energy from (5) to (8).

$$W_{ac} = - \left[\rho A L \frac{\partial^2 v(z,t)}{\partial t^2} \Big|_{z=H} + \int_0^L \rho A \frac{\partial^2 u(x,t)}{\partial t^2} dx \right] v(z,t) \Big|_{z=H} \quad (6)$$

$$u^{total}(x,t) = u(x,t) + v(z,t) \Big|_{z=H} \quad (7)$$

$$T = \left(\int_0^L \frac{1}{2} \rho A \left(\frac{\partial u(x,t)}{\partial t} \right)^2 + \rho A \frac{\partial u(x,t)}{\partial t} \frac{\partial v(z,t)}{\partial t} \Big|_{z=H} + \frac{1}{2} \rho A \left(\frac{\partial v(z,t)}{\partial t} \right)^2 \Big|_{z=H} \right) dx + \int_0^H \frac{1}{2} \rho_T A_T \left(\frac{\partial v(z,t)}{\partial t} \right)^2 dz + \frac{1}{2} M_0 \left(\frac{\partial v(z,t)}{\partial t} \right)^2 \Big|_{z=H} \quad (8)$$

Once the energy terms are defined, it is possible to obtain the energy functional (L_S):

$$L_S = \left(\int_0^L \frac{1}{2} \rho A \left(\frac{\partial u(x,t)}{\partial t} \right)^2 + \rho A \frac{\partial u(x,t)}{\partial t} \frac{\partial v(z,t)}{\partial t} \Big|_{z=H} + \frac{1}{2} \rho A \left(\frac{\partial v(z,t)}{\partial t} \right)^2 \Big|_{z=H} \right) dx + \int_0^H \frac{1}{2} \rho_T A_T \left(\frac{\partial v(z,t)}{\partial t} \right)^2 dz + \frac{1}{2} M_0 \left(\frac{\partial v(z,t)}{\partial t} \right)^2 \Big|_{z=H} - \int_0^L \frac{1}{2} EI \left(u_{,xx}^2 + u_{,xx}^2 u_{,x}^2 + \frac{1}{4} u_{,xx}^2 u_{,x}^4 \right) dx - \int_0^H \frac{1}{2} E_T I_T \left(v_{,zz}^2 + v_{,zz}^2 v_{,z}^2 + \frac{1}{4} v_{,zz}^2 v_{,z}^4 \right) dz - \int_0^L Fc(x) \left(\frac{1}{2} \left(\frac{du}{dx} \right)^2 + \frac{1}{8} \left(\frac{du}{dx} \right)^4 \right) dx - F \sin(\omega_f t) v(z,t) \Big|_{z=H} - \left[\rho A L \frac{\partial^2 v(z,t)}{\partial t^2} \Big|_{z=H} + \int_0^L \rho A \frac{\partial^2 u(x,t)}{\partial t^2} dx \right] v(z,t) \Big|_{z=H} \quad (9)$$

2.2 Inverted Pendulum

An inverted pendulum is placed at the top of the tower to act as a TMD (Fig. 2), its behavior is similar to a regular pendulum, however it requires shorter lengths to achieve equivalent performances. The pendulum has length l , mass m , rotational spring K_P and the rotational displacement is given by θ .

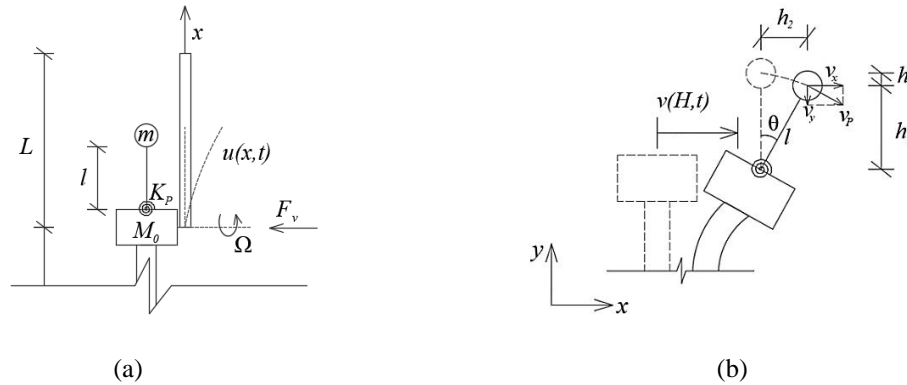


Figure 2. (a) Detail of structure with an inverted pendulum (b) inverted pendulum deformed shape

From the settings of the height h_l (10) and velocity v_p (11), it is possible to define the energy functional given

by (12), which must be added to the expression for the system functional energy.

$$h_1 = l \cos(\theta) \quad (10)$$

$$v_p^2 = \left(\frac{\partial v(H,t)}{\partial t} \right)^2 + 2l \frac{\partial v(H,t)}{\partial t} \cos(\theta) + l^2 \left(\frac{d\theta}{dt} \right)^2 \quad (11)$$

$$L_p = \frac{1}{2} m \left[\left(\frac{\partial v(H,t)}{\partial t} \right)^2 + 2l \frac{\partial v(H,t)}{\partial t} \cos(\theta) + l^2 \left(\frac{d\theta}{dt} \right)^2 \right] - mgl \cos(\theta) - \frac{1}{2} K_p \theta^2 \quad (12)$$

2.3 Modal solution

The Rayleigh-Ritz method is applied in order to obtain the structure response. Thus, the displacements of both blade and tower are assumed as:

$$u(x,t) = \sum_{j=0}^n a_j \phi_j(x), \quad v(z,t) = \sum_{j=0}^n b_j \psi_j(z) \quad j = 1..n \quad (13)$$

where a_j and b_j are time dependent coefficients, n is the number of modes of the solution and $\phi_j(x)$ and $\psi_j(z)$ are the admissible functions, which satisfy the boundary conditions, they are given by:

$$\phi_j(x) = 1 - \cos \left[\frac{(2j-1)\pi x}{2L} \right], \quad \psi_j(z) = 1 - \cos \left[\frac{(2j-1)\pi z}{2H} \right] \quad (14)$$

The Hamilton's principle is then applied, as shown by Eq. (15), to get a set of nonlinear differential equations of motion that can be solved by applying the Runge-Kutta method:

$$\frac{\partial L_s}{\partial a_j} - \frac{d}{dt} \left(\frac{\partial L_s}{\partial \dot{a}_j} \right) = F_{NC} = c \dot{a}_j \quad (15)$$

It is worth mention than F_{NC} refers to non-conservative forces that may act, especially as viscous damping, which is given by the product between velocity and damping coefficient c .

First, a free vibration solution is sought to determine the natural frequencies. Then, it is assumed that the coefficients a_j and b_j are harmonic, where ω is the natural frequency:

$$a_j(t) = \bar{a}_j e^{i\omega t}, \quad b_j(t) = \bar{b}_j e^{i\omega t} \quad (16)$$

By substituting (16) in the differential equations and disregarding the nonlinear terms, it is obtained a set of algebraic equations, which can be written in matrix form, where \mathbf{K} is the stiffness matrix, \mathbf{M} is the mass matrix and \mathbf{A} is the amplitude vector:

$$(\mathbf{K} - \omega^2 \mathbf{M}) \mathbf{A} = 0 \quad (17)$$

Equation (17) constitutes an eigenvalue problem, where ω^2 are the eigenvalues and the eigenvectors give the vibration modes. Considering a solution with 5 modes for both blade and tower, the Fig. 3a shows how the natural frequencies change with the increase in the blade rotating frequency Ω . The tower parameters considered are: height $H=46$ m, density $\rho_T=7850$ kg/m³, Young's modulus $E_T=210$ GPa, the inner tower diameter is 1.49 m and the outer diameter is 1.50 m; and the blade parameters are: length $L=22$ m, density $\rho=2770$ kg/m³, Young's modulus $E=69$ GPa, the width is 0.5 m and the thickness 0.1 m; the nacelle has a mass $M_0=30000$ kg.

Figure 3 displays the natural frequencies of blade and tower in an uncoupled and coupled situation. Figure 3(a), shows the coupled natural frequencies meanwhile Figure 3(b), displays the natural frequencies in an

uncoupled situation. It is observed that the points of intersection for the uncoupled frequencies in Fig. 3(b) match the regions A, B and C of the Fig. 3(a), where the veering phenomenon occurs. These regions are worth to investigate regarding resonance since more than one mode can produce large displacements. Furthermore, when the rotating frequency Ω increases, the natural frequency also increases, leading to the conclusion that the parked conditions ($\Omega=0$ rpm) is the one with more flexibility.

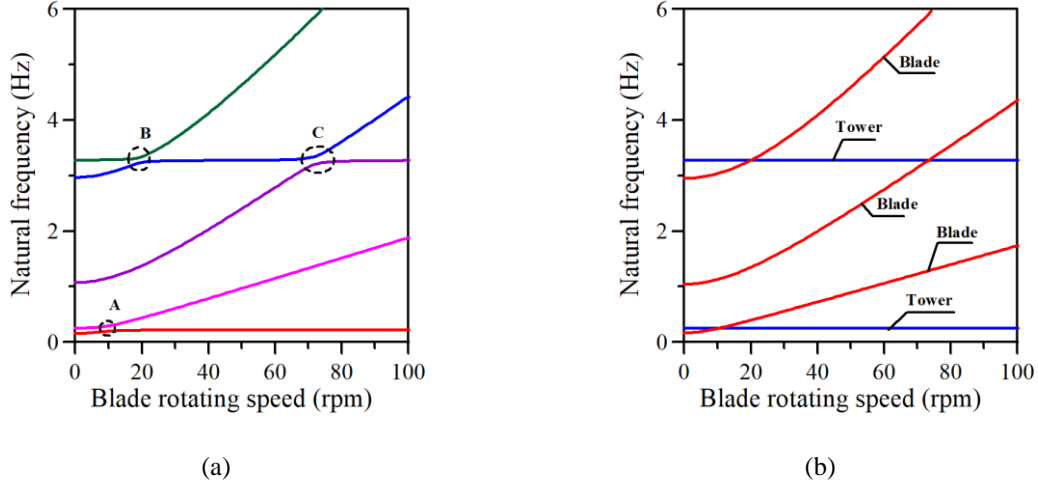


Figure 3. Natural frequencies (a) Coupled structure (b) Uncoupled structure

3 Frequency-domain response

As previously indicated, in order to control the system vibration an inverted pendulum is installed to the wind turbine and, aiming to determine the optimum parameters for this pendulum, the frequency-domain response is sought. The coefficients a_j and b_j are once again assumed as harmonic in addition to θ , due to the pendulum addition, then:

$$a_j(t) = \bar{a}_j e^{i\omega t}, \quad b_j(t) = \bar{b}_j e^{i\omega t}, \quad \theta(t) = \bar{\theta} e^{i\omega t} \quad (18)$$

The differential equations obtained from Hamilton's principle become algebraic equations when expressions (18) are substituted into them. Using a solution with three modes, the following system is obtained:

$$\left(\frac{3\rho AL}{2} - \frac{4\rho AL}{\pi} \right) \omega^2 \bar{a}_1 + \left(\rho AL - \frac{2\rho AL}{\pi} \right) \omega^2 \bar{b}_1 + c_B i \omega \bar{a}_1 + \left(\frac{\pi^2 \rho AL \Omega^2}{24} - \frac{\rho AL \Omega^2}{8} + \frac{\pi^4 EI}{32L^3} \right) \bar{a}_1 = 0 \quad (19)$$

$$\left(\frac{3\rho AL}{2} - \frac{3\rho AL}{\pi} \right) \omega^2 \bar{a}_1 + \left(\frac{3\rho AL}{2} + \frac{3\rho_T A_T H}{2} - \frac{4\rho_T A_T H}{\pi} + \frac{M_0}{2} + m \right) \omega^2 \bar{b}_1 + m \omega^2 \bar{\theta} + c_T i \omega \bar{b}_1 + \left(\frac{\pi^4 E_T I_T}{32H^3} \right) \bar{b}_1 = F \quad (20)$$

$$m \omega^2 \bar{b}_1 + m \omega^2 \bar{\theta} + c_p i \omega \bar{\theta} + K_p \bar{\theta} = 0 \quad (21)$$

The system can be solved for \bar{a}_1 , \bar{b}_1 and $\bar{\theta}$, therefore they will be written in terms of the frequency ω . Since \bar{b}_1 gives the amplitude of the tower displacement, the dynamic amplification factor (DAF) is the quotient of the module of \bar{b}_1 and the static response. Keeping the blade and tower parameters obtained from last section for the parked condition ($\Omega=0$ rpm), and using a pendulum of mass 850 kg (around 10% of the tower's mass), spring stiffness 100 kN.m/rad and length 5.15 m, Fig. 5(a) presents DAF for different damping ratios (ζ). From Fig. 5(a) it is possible to verify that the installation of the IPTMD creates two peaks around a without control peak response. That is the region where the IPTMD is aiming to have best performance. Furthermore, the structure curve with the

pendulum always intersect two points (P and Q), independently of the damping ratio. This was first observed by Den Hartog [11], who states that in the optimum condition both points have the same ordinate and also one of them is a maximum point. Therefore, an iterative process was developed searching the optimum length and damping ratio for the pendulum, keeping the other parameters constant: from a starting length it is possible to get the frequencies at P and Q (ω_P and ω_Q), then each frequency is substituted in the DAF expression generating two expressions whose subtraction has to be zero, giving a new length and a new ω_P and ω_Q and so on, until the value for the length converges. After this, to get the optimum damping ratio, it is necessary to make sure that P or Q is a maximum point by performing the derivative at this point and making it equal to zero. For the case studied the optimum length is 5.241 m and damping ratio of 11.4%, the correspondent frequency-domain response is shown in Fig. 5(b).

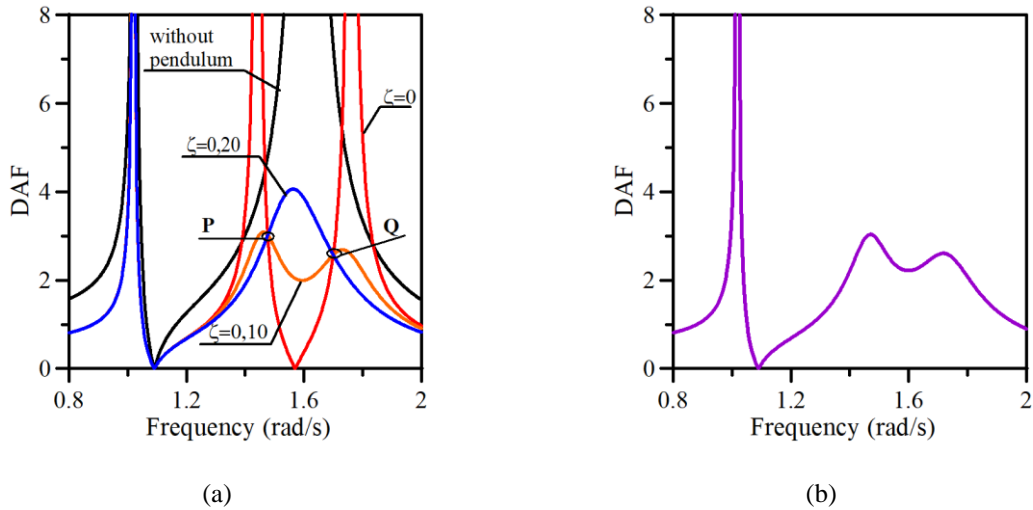


Figure 5. Frequency-domain response ($\Omega=0$ rpm) (a) for $l=5.15$ m (b) optimum condition

4 Time-domain response

The Runge-Kutta method can be applied to the differential equations of motion to get the time response of the structure. For the parked conditions, the first and second natural frequencies are, respectively, $\omega=0,99$ rad/s and $\omega=1,59$ rad/s. In order to evaluate the resonance response an harmonic force with these frequencies and intensity of 1 kN is applied. Figures 6 and 7 show the displacement of the tower top for these conditions. The pendulum parameter are the optimum ones obtained in the previous section. It is observed that the excitation of $\omega=1,59$ rad/s lead to large displacements, therefore IPTMD was tuned to that frequency aiming to control these displacements.

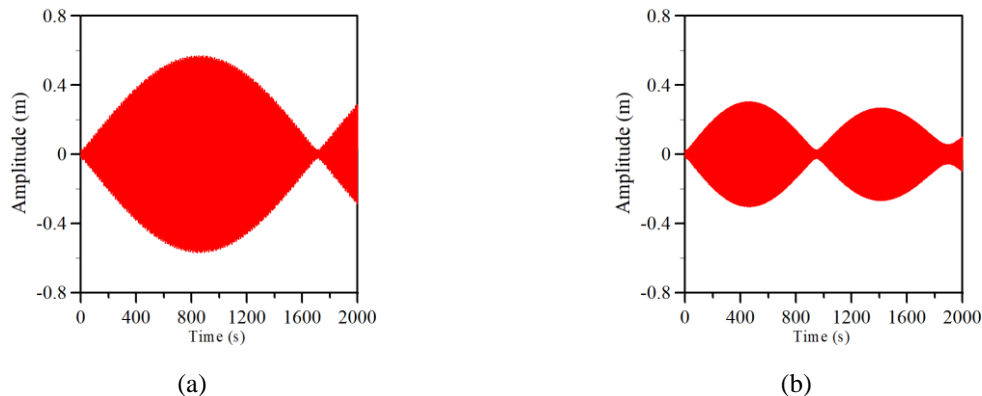


Figure 6. Time response ($\omega=0,99$ rad/s) (a) without TMD (b) with TMD

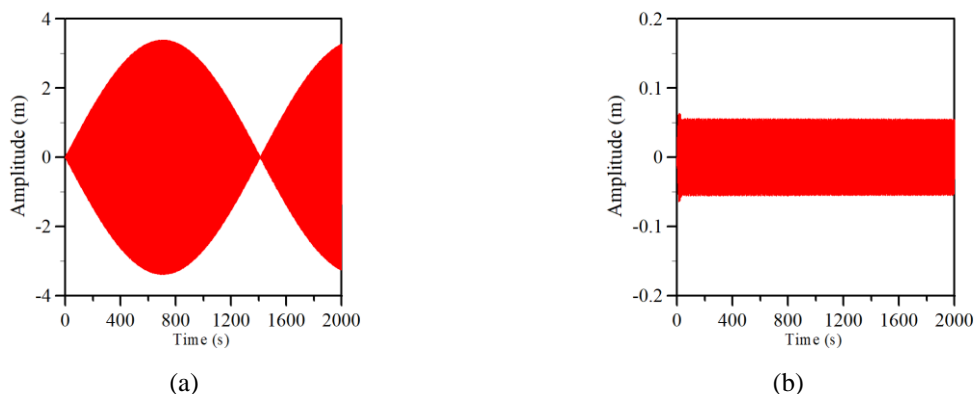


Figure 7. Time response ($\omega_f=1,59$ rad/s) (a) without TMD (b) with TMD

5 Conclusions

Therefore, the results for time-domain response show that the tower displacement with the IPTMD are kept at safe levels, however the pendulum works better under the excitation which it was tuned for ($\omega=1,59$ rad/s). The method applied to determine the optimum parameters can be used at any given rotation of the blade, thus it can work for parked and operating conditions, though further study is necessary to verify if a single IPTMD could be effective for a wide range of excitations and blade rotation velocities.

Acknowledgements. The research described in this paper was financially supported by the Coordination for the Improvement of Higher Education Personnel (CAPES). In addition, I would like to thank the postgraduate program in geotechnics, structures and civil construction (PPG-GECON-UFG).

Authorship statement. The authors hereby confirm that they are the sole liable persons responsible for the authorship of this work, and that all material that has been herein included as part of the present paper is either the property (and authorship) of the authors, or has the permission of the owners to be included here.

References

- [1] SOONG, T.T; DARGUSH, G.F. *Passive energy dissipation systems in structural engineering*, Chichester: John Wiley & Sons, 1997.
- [2] MURTAGH, P. J.; GOSH, A.; BASU, B.; BRODERICK, B. M. "Passive control of wind turbine vibrations including blade/tower interaction and rotationally sampled turbulence". *Wind Energy*, v 11, p. 305-307, 2008.
- [3] FARSADI, T.; KAYRAN, A. "Structural dynamics analysis and passive control of wind turbine vibrations with Tuned Mass Damper (TMD) technique". In: *57th AIAA/ASCE/AHS/ASC Structures, Structural Dynamics, and Materials Conference, 2016, San Diego, California. Proceedings ... USA: American Institute of Aeronautics and Astronautics*, 2016.
- [4] ZUO, H.; BI, K.; HAO, H. "Using multiple tuned mass dampers to control offshore wind turbine vibrations under multiple hazards". *Engineering Structures*, v 141, p. 303-315, 2017.
- [5] ORLANDO, D. *Absorvor pendular para controle de vibrações de torres esbeltas*. Dissertação (Mestrado em Engenharia Civil), Pontifícia Universidade Católica do Rio de Janeiro, 2006.
- [6] GUIMARÃES, P. V. B.; MORAIS, M. V. G.; AVILA, S. M. "Tuned Mass Damper inverted pendulum to reduce offshore Wind turbine vibrations". In: *VETOMAC X (2014), Vibration Engineering and Technology of Machinery*, p. 379-388. - TIRAR
- [7] SUN, C.; JAHANGIRI, V. "Bi-directional vibration control of offshore wind turbines using a 3D pendulum tuned mass damper". *Mechanical Systems and Signal Processing*, v 105, p. 338-360, 2018.
- [8] RESENDE, DIOGO V. ; DE MORAIS, MARCUS V. G. ; AVILA, SUZANA M. "Experimental Analysis of One-Degree-of-Freedom (1DoF) Dynamic System Controlled by Optimized Inverted Pendulum". *Journal of Vibration Engineering & Technologies*, v. 8, p. 1-13, 2020.
- [9] KANG, N.; PARK, S.C.; PARK, J. ATLURI, S. N. "Dynamics of flexible tower-blade and rigid nacelle system: dynamic instability due to their interactions in wind turbine". *Journal of Vibration and Control*, p.1-11, 2014.
- [10] MEIROVITCH, L. *Fundamentals of vibrations*. 1 ed. New York: McGraw-Hill, 2001.
- [11] DEN HARTOG, J. P. *Mechanical vibrations*. 3. ed. New York: McGraw-Hill, 1947.